AIAA SciTech Forum
6-10 January 2025, Orlando, FL
AIAA SCITECH 2025 Forum

10.2514/6.2025-0844

Acoustic Testing of the Joby Aviation Propeller in the National Full-Scale Aerodynamics Complex 40- by 80-Foot Wind Tunnel

Natasha L. Schatzman* and Lauren Weist †
NASA Ames Research Center, Moffett Field, CA, 94043, USA

Jeremy J. Bain‡ and Austin D. Thai §
Joby Aviation, Santa Cruz, CA, 95060, USA

The advanced air mobility sector has progressed in recent years with electric vertical take-off and landing vehicles at the forefront. In response, the NASA Advanced Air Mobility (AAM) project has initiated the AAM National Campaign to partner with industry to progress this emerging market. This resulted in NASA's Revolutionary Vertical Lift Technology project electing to participate in experimental efforts to develop datasets for computational tool validation for these AAM vehicle configurations. AAM vehicles can gain wide adoption if there is sufficient community acceptance; and for community acceptance noise has been identified as a critical obstacle to achieve success in this emerging market. To further understand electric vertical take-off and landing vehicle noise, an isolated Joby Aviation S4 propeller was tested in the National Full-Scale Aerodynamics Complex 40- by 80-Foot Wind Tunnel at NASA Ames Research Center to aid in providing high quality performance, loads, and acoustic data. Details of test hardware and setup are described with a focus on acoustics, which includes facility, test model, microphone locations, and data acquisition system details. Additionally, the data processing techniques and completed test matrix for acoustic points are provided. To aid in identifying potential acoustic reflections, an acoustic reflection test was performed prior to the start of the test and highlighted the presence of reflections at every microphone location. Acoustic results are provided for various flight regimes for sweeps of blade pitch, RPM, flow angle, and wind speed. These results show an optimum RPM for a specific thrust level for noise, and further reductions in RPM can increase noise levels. This dataset will be used to evaluate and improve computational tools within the NASA RVLT Conceptual Design Toolchain.

Nomenclature

AAM	=	advanced air mobility
DAQ	=	data acquisition
EPU	=	electric propulsion unit
eVTOL	=	electric vertical take-off and landing
FFT	=	fast Fourier transform
ISPL	=	integrated sound pressure levels
NFAC	=	National Full-Scale Aerodynamic Complex
RPM	=	revolutions per minute
RVLT	=	Revolutionary Vertical Lift Technology
SPL	=	sound pressure level, dB ref. 20 µPa
TTL	=	transistor-transistor logic
UAM	=	urban air mobility
VKF	=	Vold-Kalman filter
V_∞	=	wind tunnel speed, m/s

*Aerospace Engineer, Aeromechanics Branch
†Aerospace Engineer, Aeromechanics Branch
‡CFD and Aeroacoustics Lead, Flight Physics
§Acoustics Senior Engineer, Flight Physics

α_p = propeller angle of attack or turntable yaw angle (axial: 0 deg, edgewise: 90 deg), deg
θ_0 = propeller blade pitch, deg

I. Introduction

Emerging advanced air mobility (AAM) vehicle configurations and technologies have pushed researchers to increase their understanding of the unique aerodynamic and aeroacoustic phenomena associated with these new designs. To address these challenges, the NASA AAM Project initiated the AAM National Campaign to partner with industry to progress this emerging market [1]. This effort further resulted in NASA's Revolutionary Vertical Lift Technology (RVLT) project to also participate in experimental efforts for computational tool validation for AAM vehicle configurations.

The Joby Aviation S4 aircraft is an electric Vertical Take-Off and Landing (eVTOL) vehicle with six tilting propulsion stations each with a 5-bladed composite variable pitch propeller. The Joby Aviation production prototype S4 aircraft is shown in Fig. 1. A summary of specifications include the ability to carry a pilot plus up to four passengers, with a 100-mile range at a maximum speed of 90 m/s (175 knots). In 2021, Joby Aviation performed a flight test on their pre-production eVTOL prototype for the AAM National Campaign over representative conditions for all phases of a typical mission profile over a large microphone array with support from NASA [1]. While flight testing is an essential tool for measuring full aircraft values, a controlled wind tunnel test of a single propeller allows for high-fidelity data to be available for design evaluation and validation. Consequently, an isolated Joby Aviation S4 propeller was tested in the National Full-Scale Aerodynamic Complex (NFAC) 40- by 80-Foot Wind Tunnel in 2023 with Air Force Agility Prime and NASA support.

Fig. 1 Joby Aviation production prototype S4 aircraft.

Test objectives for NASA included providing NASA projects with high quality acoustic data to support the AAM National Campaign and further validate software within the RVLT project's conceptual design toolchain, increasing the understanding of urban air mobility (UAM) noise [2]. Joby Aviation's objectives were to obtain high-fidelity performance, loads, and acoustics of its propeller across a wide range of representative flight conditions. Under the terms of the agreement between the partners, limited information regarding microphone position, blade geometry, flight conditions, and data is provided in this paper.

II. Test Hardware and Setup

Test hardware and setup are described in terms of the facility, test apparatus, microphone locations, data instrumentation, and acquisition system set up. In summary, an isolated Joby Aviation S4 propeller was tested in the NFAC 40- by 80-Foot Wind Tunnel surrounded by 20 strut mounted microphones and 8 floor mounted microphone arrays to capture the acoustic radiation from the propeller.

A. Facility

An isolated Joby Aviation S4 propeller was tested in the NFAC 40- by 80-Foot Wind Tunnel located at NASA Ames Research Center in Moffett Field, California. The NFAC 40- by 80-Foot Wind Tunnel is a closed circuit, closed test-section facility with semicircular sides and driven by six electrically powered, 40-foot diameter, 12-bladed, variable-pitch and variable-RPM fans. The tunnel's maximum wind speed is 154 m/s (300 knots, 347 MPH) and has a rotating turntable with the ability to yaw a model up to 180 degrees. The stagnation pressure in the wind tunnel test section is atmospheric, and the temperature is uncontrolled and dependent on the outdoor temperature [3]. The testing facility was chosen due to its ability to conduct full scale propeller tests and history of various acoustic tests, including a Bell 699 rotor on the Tiltrotor Test Rig and the Aerodynamic and Acoustic Rotorprop Test program [4, 5]. The tunnel is currently operated by the U.S. Air Force's Arnold Engineering Development Complex.

The test section of the the NFAC 40- by 80-Foot Wind Tunnel is treated with acoustic lining on the walls, floor, and ceiling, with most areas containing a 42-inch-deep liner that provides an absorptivity of greater than 90% at frequencies above 100 Hz [6]. This treatment reduces the usable test section to 39 by 79 feet, but greatly increases its acoustic capabilities. It is important to note that the turntable and some parts of the ceiling are less effective, and only absorbs 78% of the acoustic energy (i.e. only 6.6 dB attenuation) below 315 Hz due to the turntable mechanisms reducing the available space for acoustic treatment [3].

B. Test Apparatus

The isolated Joby Aviation wing-tip propulsion unit with a 5-bladed composite propeller and spinner were mounted on an NFAC-provided sting in the NFAC 40- by 80-Foot Wind Tunnel on the turntable as shown in Fig. 2. The sting mount consisted of the spool stack, pitch head, sting, and force balance. Power and data cable to the Electric Propulsion Unit (EPU), force balance, and other non-rotating instrumentation were routed along the outer surface of the sting and spool stack. The propeller was powered by a 250 kW Gustav-Klein high voltage direct current bidirectional power supply.

Mounting on the turntable allowed the propeller to be yawed from 0 to 180 degrees, which is denoted as flow angle (α_p). Furthermore, the propeller RPM and blade pitch (θ_0) were adjustable. To aid in the suppression of vortex shedding noise from the model sting mount, the vertical sting component was wrapped with wire in a helical formation and can be seen in Fig. 2 [7].

C. Microphone Placement

A total of 20 strut-mounted microphones and 8 floor-mounted microphone phased arrays were installed around the propeller, see Fig. 2. Microphones 1 through 8 were installed on two 10-foot struts mounted on the turntable to capture in-plane noise and were counter-yawed as the turntable yawed to ensure that the microphones were always facing into the wind for all flow angle positions. Microphones 9 through 20 were installed on three 15-foot struts and mounted off turntable to capture out-of-plane noise, and did not move spatially or rotate when the turntable was yawed. Microphone phased arrays 21 through 28 were flush mounted on the turntable. All microphone struts were designed using the McMasters-Henderson airfoil in order to minimize vortex tone noise and flow interference [8].

A graphical top and side view of the isolated Joby Aviation aircraft propeller and microphone locations for the edgewise flight configuration (α_p = 90 degrees) is shown in in Fig. 3. For reference, an elevation angle of 0 degrees denotes the horizon plane and -90 degrees is directly below the propeller. In edgewise flight, microphones #1 and #19 are located at an elevation angle of +1.8 and -36.6 degrees, respectively. In hover, microphones #1 and #19 are located at an elevation angle of +1.8 and +42.6 degrees, respectively.

D. Data Instrumentation and Acquisition

Free-field GRAS 40AC 1/2" microphones with GRAS 26AJ 1/2" preamplifers and GRAS 1/2" nose cones were used for strut mounted microphones 1 through 20. These microphones were powered by three GRAS 12AG 8-channel power modules and connected by Lemo 7-pin cables. The microphone channel gains on the power supply were set and recorded prior to the start of each data point to ensure the signal was at a proper magnitude to avoid electrical interference and the linear-response signal conditioning setting was chosen to capture all frequencies. The power supply was connected to a Dewetron Trendcorder DAQ. Each data point was induced by a trigger signal from the Joby team. The DAQ recorded acoustic signals from the 20 strut mounted microphones, 8 single microphones from the phased arrays (as close to the center of the array as possible), a one-per-rev Transistor-Transistor Logic (TTL) pulse signal, a

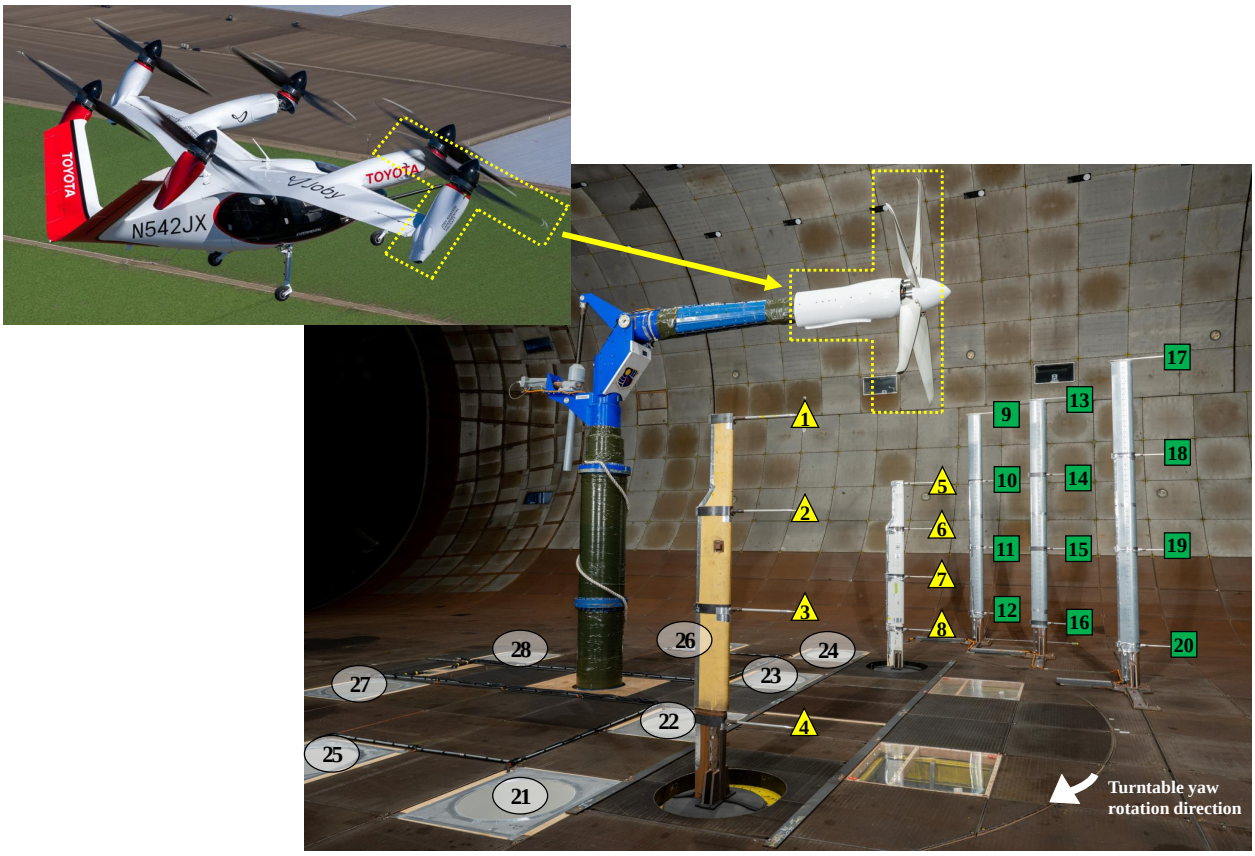

Fig. 2 Joby Aviation Production Prototype S4 aircraft and isolated Joby Aviation aircraft propeller in the NFAC 40- by 80-Foot Wind Tunnel with microphone placement location.

run number signal, and a point number signal. The microphone power supplies and NFAC signals were connected to the DAQ via BNC cables and the DAQ was time-synced to the Joby and NFAC systems via an Ethernet connector.

An end-to-end calibration of each microphone channel was performed weekly using a fixed-frequency pistonphone (G.R.A.S. Type 42AA) of known output (nominally 114 dB at 250 Hz) to ensure an accurate engineering unit conversion calibration factor. Small corrections for variations in atmospheric pressure at the test location (sea level) were included in the calibration.

The strut-mounted and phased array microphones were acquired on two different NASA DAQ systems, see Fig. 4. Data were acquired at a sampling rate of 200 kHz and 96 kHz for the strut-mounted and phased array microphones, respectively. The data collection start time was triggered by Joby Aviation's system and acquired for 30 seconds. A one-per-revolution signal was provided by the NFAC 40- by 80-Foot Wind Tunnel system for all blades on points.

Non-acoustic instrumentation systems included the NFAC BDAS data system, a Joby Data Acquisition System, the LORD Telemetry System, and the Joby High Resolution Recorder (HRR). The test article was controlled using a Joby LabView GUI and by a Joby DAQ manager, while the NFAC Wind Tunnel was operated independently from all Joby systems.

III. Data Processing

All acoustic data was processed using MATLAB R2023a with the signal processing toolbox [9]. Data was first transferred from the Dewetron Trendcorder DAQ to a PC in .dmd format and converted to .mat within MATLAB. The microphone calibration factor was applied to convert the time history data from Volts to Pascals, along with the set gain value applied. The Welch method was performed using a half-second spectral averaging technique with 50% overlap [10]. The Welch method is the process of splitting up the time history into equal segments and performing a Fast Fourier Transform (FFT) on each segment and averaging all individual segments together. Due to additional

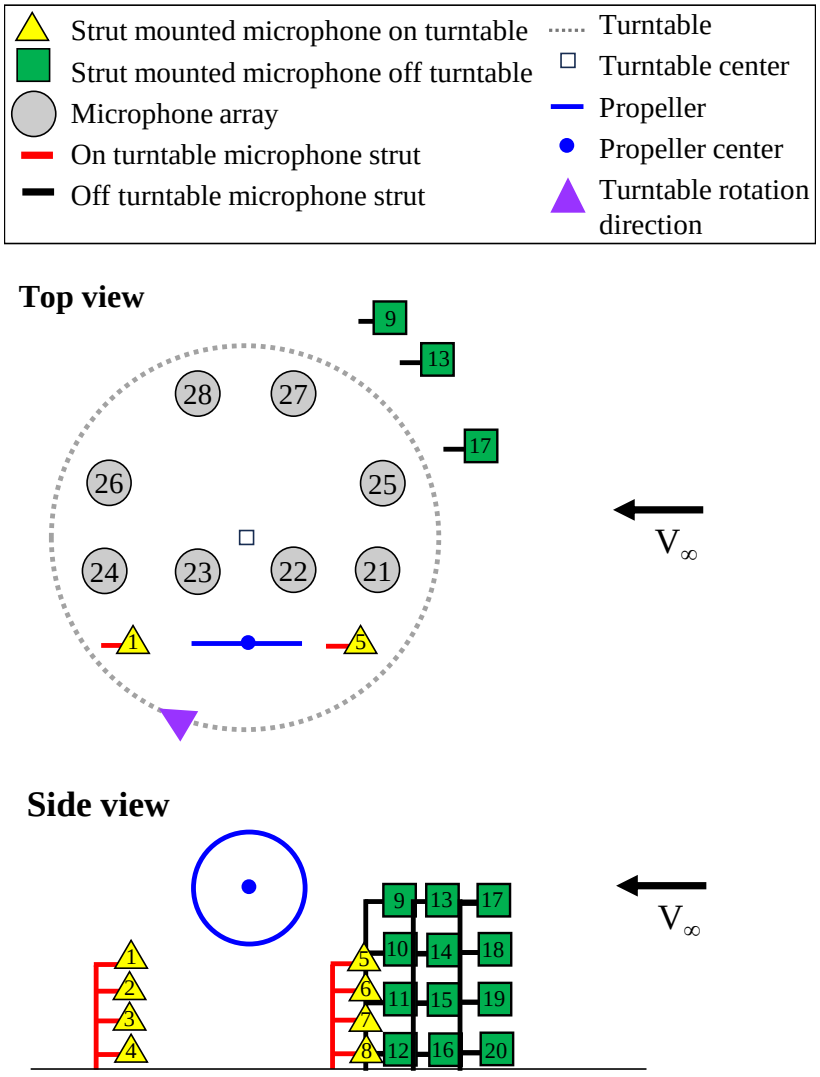

Fig. 3 Graphical top and side view of the propeller and microphones for the edgewise flight configuration.

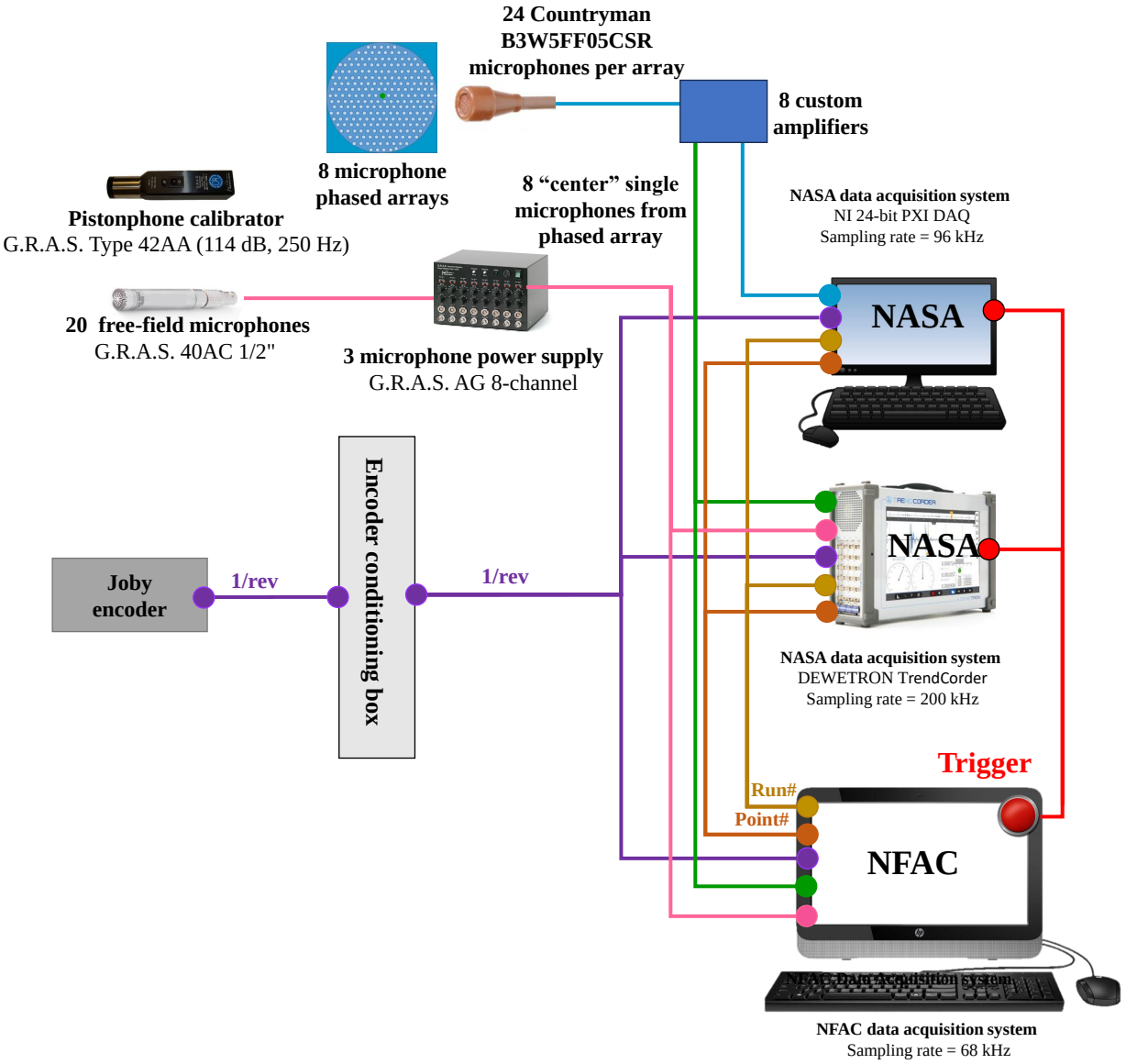

Fig. 4 Acoustic data acquisition and equipment setup.

non-tunnel background noise from the Joby hardware used during the test, a Vold-Kalman filter (VKF) was applied to compute the non-propeller shaft-coherent acoustic content [11]. The difference between the original pressure time history and the pressure time history of the non-propeller shaft-coherent acoustic content is denoted as the "filtered" data. This provides a better representation of the propeller acoustic content, and yields greater insight into the propeller noise sources. Prior work applying the VKF to Joby aircraft acoustic flight test measurements were successful [12, 13]. A summary of the acoustic data processing procedure is shown in Fig. 5.

To highlight the significance of VKF processing effort, unfiltered data and data filtered with the VKF are shown in Figs. 6a and 6b for microphones #1 and #19, respectively, for a hover condition at a blade pitch of 27 degrees for blades on, blades off, and tunnel background conditions. 'Blades on' refers to the test model with blades installed and spinning with the cooling fan on. 'Blades off' refers to a bare hub spinning without blades installed with cooling fan on. Unfiltered tunnel background refers to blades off and cooling fan off to highlight the NFAC 40- by 80-Foot Wind Tunnel

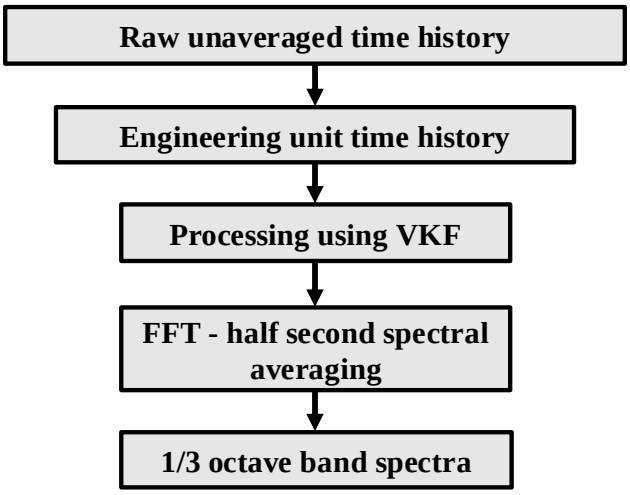

Fig. 5 Acoustic data processing procedure.

background noise without any Joby components on and wind tunnel wind off (V_∞ = 0 m/s). The application of the VKF effectively eliminated non-propeller sources within the frequency range of 500 to 10 kHz. Data for blades off is shown to highlight that propeller sources are preserved with use of the VKF application. Furthermore, the unfiltered background noise highlights additional noise sources from other components, be they Joby or NFAC in origin. Acoustic spectra is presented in the 1/3 octave band (x-axis) with major ticks marking at Δ10 dB (y-axis) for a frequency range from 20 Hz to 20 kHz.

IV. Test Matrix

A. Reflection Test Conditions

Test conditions are discussed for the reflection tests, blades off noise measurements, and the main test. Conditions for the reflection tests (wind off) are discussed in terms of turntable setting (α_p) and noise source. Blades off noise conditions are provided in terms of V_∞, α_p, and RPM with no blades on the Joby propeller. Finally, blades on conditions are presented in terms of V_∞, α_p, RPM, and θ_0. Repeated points for each test matrix are not presented, but were performed for data quality purposes.

Reflection test #	1	2	3
α_p (deg)	0 : 10 : 130	0 : 10 : 130	0 : 10 : 130
Noise source	None Equalized pink noise Balloon pop	None Equalized pink noise Balloon pop	None Equalized pink noise Balloon pop
Hardware	Reference microphone Pole microphone struts	Reference microphone Microphone struts 8 plywood panels	Reference microphone Microphone struts 8 microphone arrays Joby model and sting

Table 1 Reflection tests 1, 2, and 3 matrix summary.

Prior to the start of the test, three acoustic reflection tests were conducted with increasing hardware build-up with the goal of identifying acoustic reflections at microphone locations for the test configuration, see Figs. 7a through 7c. Each reflection test was performed in a closed tunnel with the wind off. To ensure consistency between each test, a reference

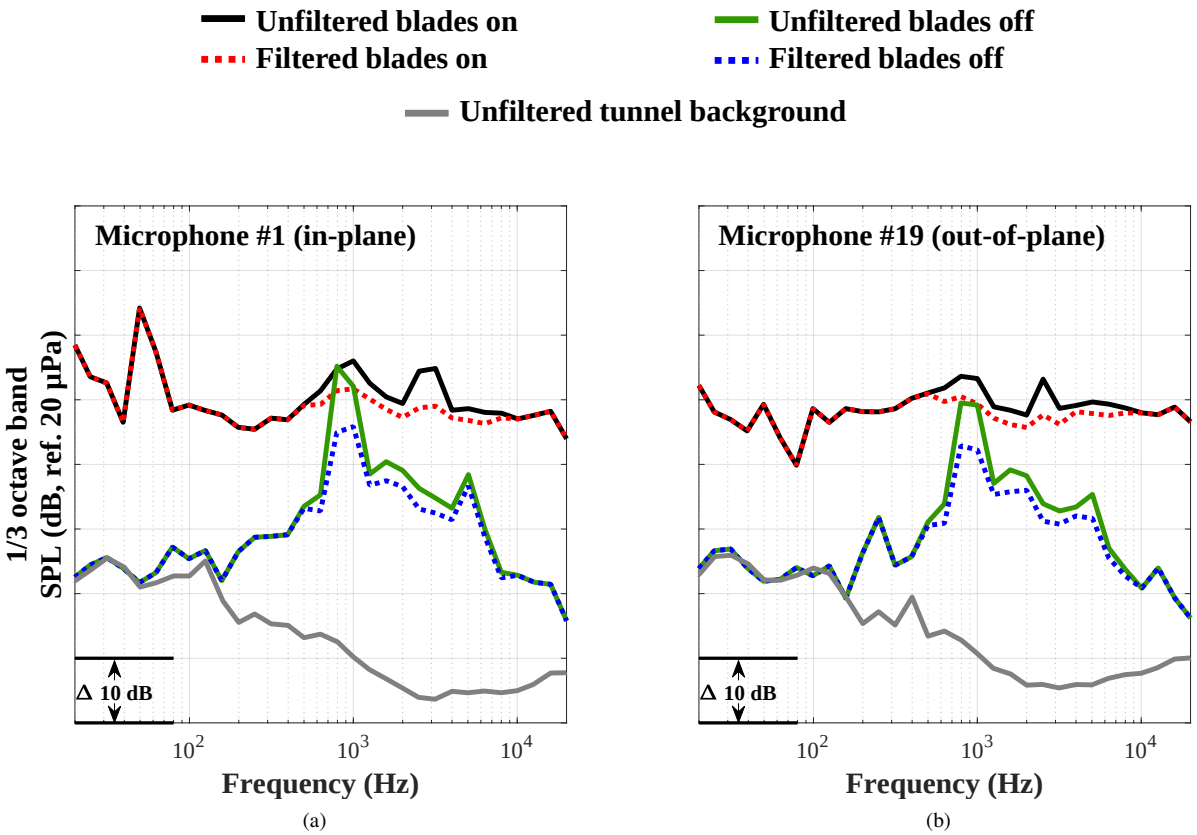

Fig. 6 Vold-Kalman filter comparison for a) in-plane microphone #1 and b) out-of-plane microphone #19 for hover data point unfiltered and filtered with blades on and off and unfiltered tunnel background noise (V_∞ = 0 m/s, θ_0 = 27 degrees, α_p = 0 degrees).

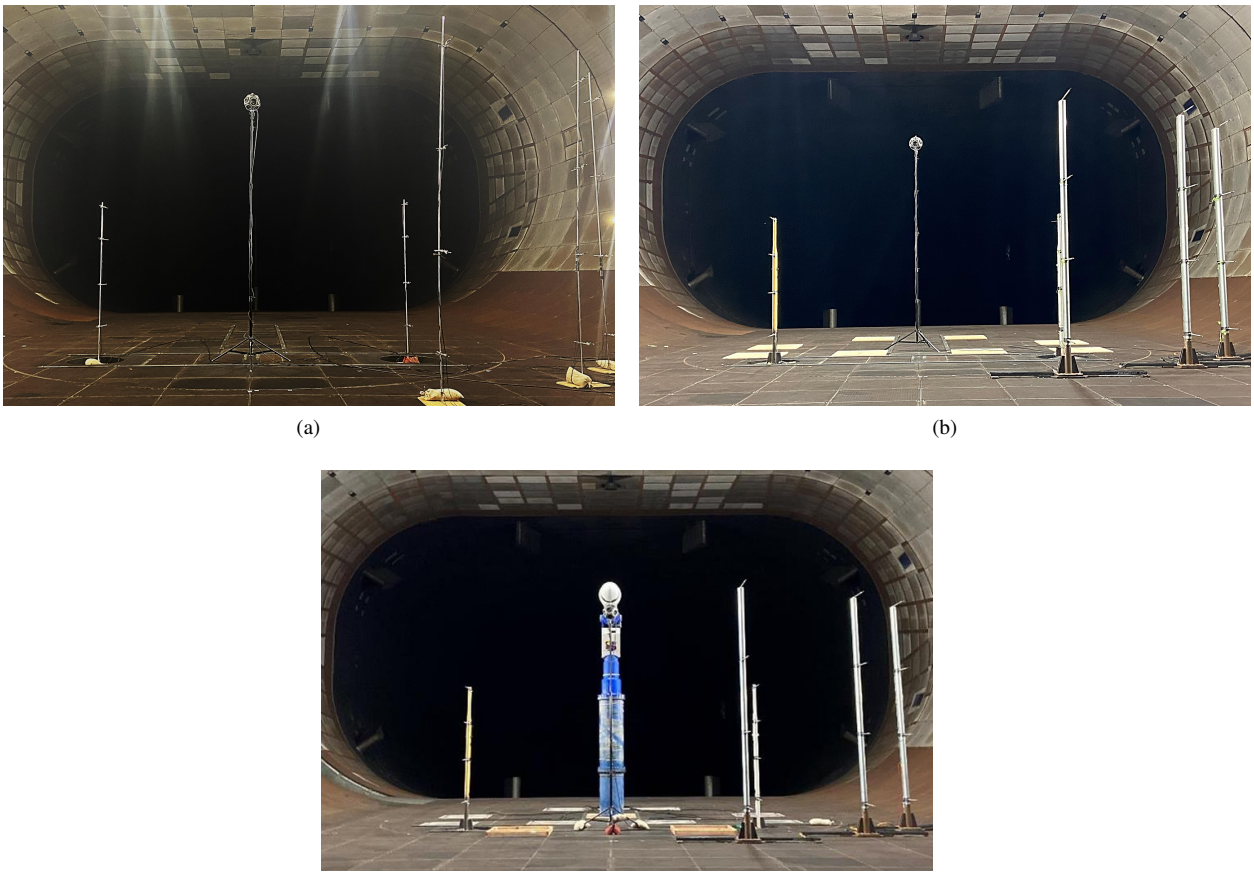

(a) (b)

(c)

Fig. 7 Reflection a) test 1, b) test 2, and c) test 3.

microphone was installed 3 feet from the wind tunnel wall in-plane with propeller hub. The reference microphone was used as a constant observer and was untouched (but calibrated) for reflection tests 1 through 3. Reflection test 1 (Fig. 7a) consisted of a closed tunnel with the reference microphone and 5 pole microphone struts installed to hold the 20 microphones at the desired microphone locations. For reflection test 2 (Fig. 7b), an addition of the microphone struts and 8 plywood panels to represent the microphone arrays were installed. Reflection test 3 (Fig. 7c) consisted of the addition of the Joby model and sting (minus propeller blades) and the 8 microphone arrays.

For each reflection test, 13 turn table locations, from 0 to 130 degrees in 10 degree increments, were selected along with two different noise sources placed at the propeller hub center. The first source was a DS3 Dodecahedron Speaker with a PA3 Power Amplifier that produced equalized pink noise with an output of 26.5 Volts. The second source was a balloon pop that served as a sharp impulsive noise to aid in identifying reflections via ray tracing. The balloon pop apparatus was manually operated within the tunnel and timing of balloon pop was coordinated between the DAQ operator and balloon pop operator. Furthermore, a quiet tunnel point was acquired for each turn table location for data quality repeatability. See Table 1 for a summary of the reflection test 1, 2, and 3 matrix.

B. Blades Off Noise Conditions

Prior to the start of the test, blades off noise measurements were acquired to aid in signal-to-noise evaluation for all test conditions. Blades off noise included a combination of wind noise over the test hardware and microphones, propeller motor, cooling fan, and tunnel drive noise. Blades off noise for a sweep of RPM, turntable yaw, and wind speed is provided in the subsequent figures. Only values for V_∞, α_p, and RPM are provided. RPM denotes the hub spinner rotational rate, and θ_0 is not provided since blades are not installed. Values of RPM are denoted in qualitative terms of low to high within this paper. Blades off noise conditions captured included hover (α_p = 0 degrees, V_∞ = 0,

RPM low to high), axial flight (α_p = 0 degrees, V_∞ = 5 to 35 m/s, RPM low to high), transition (α_p = 5 to 130 degrees, V_∞ = 5 to 35 m/s, RPM low to high), and pure edgewise flight (α_p = 90 degrees, V_∞ = 5 to 35 m/s, RPM low to high). See Table 2 for a summary of the blades off noise test matrix.

Flight Regime	V_∞ (m/s)	α_p (deg)	RPM
Hover	0	0	low to high
Axial	5 to 35	0	low to high
Transition	5 to 35	0 to 130	low to high
Pure Edgewise	5 to 35	90	low to high

Table 2 Blades off noise test matrix summary.

C. Blades On Test Conditions

A summary of the blades on propeller test condition includes a range of flight regimes including hover, axial, transition, and edgewise flight conditions; see Table 3 for a test matrix summary. Due to facility acoustic limitations, microphone stand structure limitations, and the low magnitude sound of the Joby Aviation propeller, wind tunnel speeds were limited to 30 m/s. This ensured that structural limitations and signal-to-noise requirements were adequately met. The test matrix included a range of V_∞ from 0 to 30 m/s in 10 m/s increments, α_p from 0 to 180 degree, θ_0 from -4 to 65 degrees, and RPM variation from low to high. Flight regimes tested include hover (α_p = 0 degrees, V_∞ = 0), axial flight (α_p = 0 degrees, V_∞ = 10 to 30 m/s), transition (α_p = 5 to 130 degrees, V_∞ = 10 to 30 m/s), and pure edgewise flight (α_p = 90 degrees, V_∞ = 0 to 30 m/s). Sweeps were performed on V_∞, RPM, θ_0, and α_p where applicable.

Flight Regime	V_∞ (m/s)	α_p (deg)	RPM	θ_0 (deg)
Hover	0	0	low to high	-4 to 29.5
Axial	10 to 30	0	low to high	-4 to 65
Transition	10 to 30	0 to 180	low to high	-4 to 65
Pure Edgewise	10 to 30	90	low to high	-4 to 19

Table 3 Test matrix summary.

V. Results

An overview of results from the reflection tests is provided to highlight potential reflections within the tunnel. For the test campaign, results for hover, transition, and edgewise flight are presented. For hover, results presented include a hover pitch and RPM sweep, along with a study on the effect of constant thrust for varying RPM and blade pitch angles. For transition and edgewise flight, the effect of propeller angle of attack on noise level is presented and a wind speed sweep in transition is presented.

Only results from microphones #1 and #19 are provided to highlight in-plane and out-of-plane positions from the source. Microphone #1 is located on the turntable and therefore the distance from the observer to source does not change with turntable yaw (α_p), unlike microphone #19, which does not move in absolute space. Acoustic data from the reflection tests are presented in terms of autocorrelation versus time, while results from the main test are provided in acoustic spectra in terms of 1/3 octave band (x-axis) with major ticks marking at Δ 10 dB (y-axis) for a frequency range from 20 Hz to 20 kHz. Furthermore, blades off noise data is provided in the subsequent figures to aid in signal-to-noise evaluation.

A. Reflection Test

To highlight potential reflections, acoustic results from the equalized pink noise source were processed using the autocorrelation method to identify time and intensity of reflection(s) [14]. Results from the balloon pop reflection test conditions are not presented at this time but were recorded. Autocorrelation results for reflection tests 1, 2, and 3 for α_p

= 40 degrees for microphone #1 and #19 are shown in Figs. 8a and 8b, respectively. Another yaw position is presented to highlight the changing observer to source for microphones off the turntable, see Figs. 8c through 8d for α_p = 90 degrees. Comparing α_p = 40 degrees to α_p = 90 degrees shows that the microphone off the turntable (microphone #19) contain a larger time shift in reflection due to the change in distance from the observer to source, compared to microphone #1. In summary, the time of reflection does not change for microphones on the turntable, but changes for microphones off the turntable due to changes in distance between source and observer.

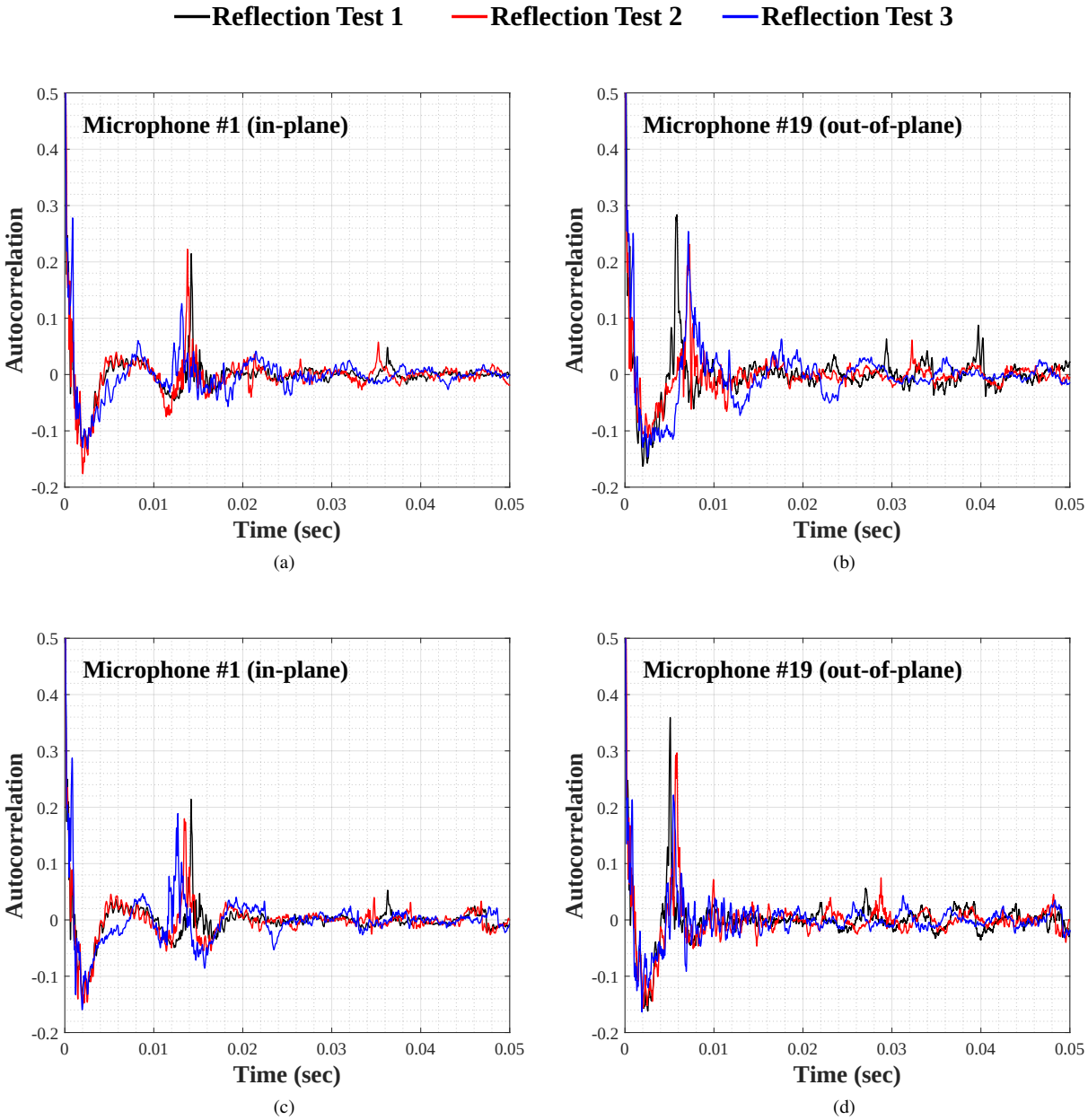

Fig. 8 Autocorrelation results for reflection tests 1, 2, and 3 for α_p = 40 degrees for a) microphone #1 and b) microphone #19 and for α_p = 90 degrees for c) microphone #1 and d) microphone #19.

The reflection test highlighted the presence of reflections for every microphone and turntable location, which could be due to turntable acoustic liner limitations, microphone/model strut hardware, deterioration of the current acoustic

liner, and camera port windows. Results reveal that caution should be taken while analyzing results and performing validations.

B. Hover

A hover pitch sweep was performed for θ_0 from -4 to 27 degrees and is shown in Figs. 9a and 9b along with blades off noise denoted by the dotted black line. Inadequate signal-to-noise is seen approximately between 600Hz and 1.2 kHz and should be viewed with caution for both microphone #1 and #19. For both microphones, as propeller blade pitch increases from 5 to 27 degrees the tonal (low to mid frequency range) and broadband (mid to high frequency range) levels increase in general. Tonal noise is more prominent (particularly around 50 Hz) for the in-plane microphone due to lower contributions of loading and broadband noise sources. For both microphones at a blade pitch of -4 degrees, an increase in loading noise (100Hz to 1 kHz) is observed. This phenomenon may be attributed to blade wake interactions at the lower thrust levels as evidenced by the increased levels at the out-of-plane microphone. An increase in broadband noise between 15 and 20 kHz is observed for blade pitches from -4 and 13 degrees for both microphone locations.

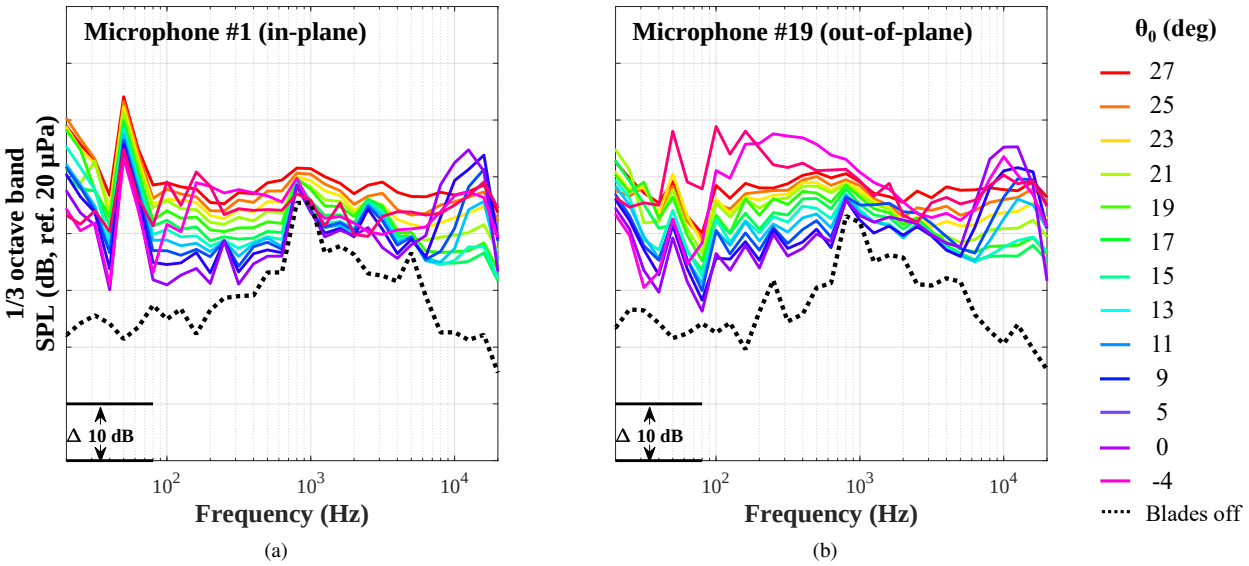

Fig. 9 Hover pitch sweep for a) in-plane microphone #1 and b) out-of-plane microphone #19 (V_∞ = 0 m/s, θ_0 = -4 to 27 degrees, α_p = 0 degrees).

A RPM sweep was performed for a constant blade pitch of 11 degrees as shown in Figs. 10a and 10b. For simplification, blades off noise provided is at the highest RPM. Similar to Figs. 9a and 9b, inadequate signal-to-noise is seen between 600Hz and 1.2 kHz, particularly at the lowest RPM conditions. A general trend for both the in-plane and out-of-plane microphone is that of increasing tonal and broadband levels with increasing RPM. Tonal noise is more prominent for the in-plane microphone compared to the out-of-plane microphone with a difference of approximately 15 dB at the maximum RPM peak between 50 and 100 Hz. In general, the out-of-plane microphone reveals a higher trend in loading and broadband noise levels compared to the in-plane microphone due to the unsteady loading noise increasing with the tip Mach number.

A study was performed for the impact on propeller noise by RPM and blade pitch for a constant thrust (within 3%) hover condition, see Figs. 11a and 11b. For simplicity, blades off noise was selected for the highest RPM. In general, as RPM increases, the blade pitch must decrease to achieve the same thrust for non-stall conditions. For both in-plane and out-of-plane microphones, an increase in noise is observed due to the increase in thickness and steady loading noise with an increase in RPM or tip Mach number. For the in-plane microphone, between 100 Hz and 2 kHz, noise levels increase with increasing blade pitch angles and decreasing RPM, which is not apparent for the out-of-plane microphone. Further analysis and use of computational tools could provide insight into exact contributions of the various noise sources with varying RPM and blade pitch.

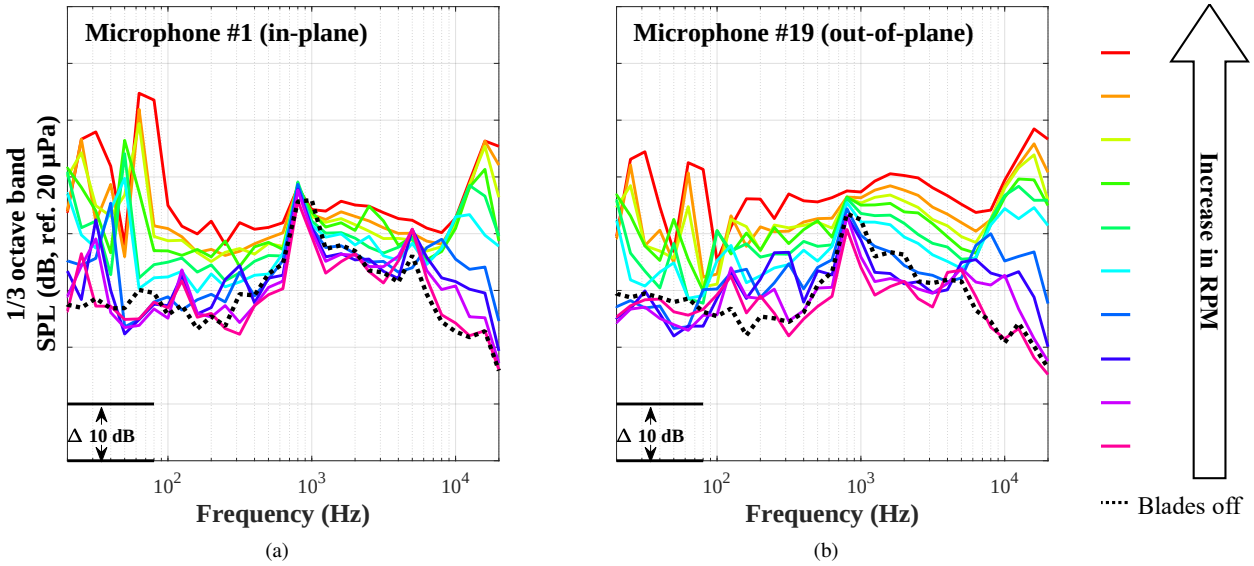

Fig. 10 Hover RPM sweep for a) in-plane microphone #1 and b) out-of-plane microphone #19 (V_∞ = 0 m/s, θ_0 = 11 degrees, α_p = 0 degrees).

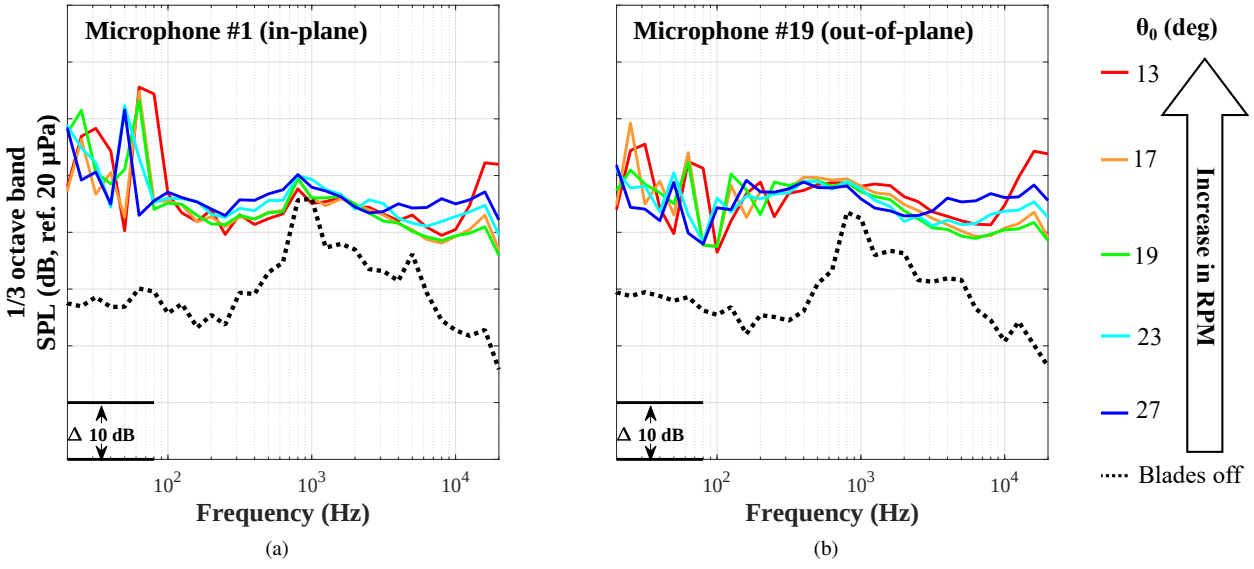

Fig. 11 Hover for constant thrust for varying RPM and pitch for a) in-plane microphone #1 and b) out-of-plane microphone #19 (V_∞ = 0 m/s, θ_0 = 13 to 27 degrees, RPM = high to low, α_p = 0 degrees).

C. Transition and Edgewise

The effect of propeller angle of attack on acoustics was explored at a wind speed of 10 m/s at a constant blade pitch of 11 degrees for α_p from 90 to 130 degrees, see Figs. 12a and 12b. Blades off noise is presented for only the the 90 and 130 degree flow angle, as there were minimal differences in blades off noise between the two angles. As previously mentioned, the variation in propeller angle-of-attack (or α_p) was achieved by rotating the turntable, which resulted in a fixed azimuth and elevation for the in-plane microphone while the out-of-plane microphone azimuth and elevation angle changed with turntable position. The α_p = 90 degrees condition corresponds to pure edgewise flow and angles-of-attack above 90 deg are indicative of negative free stream inflow, which could be representative of descending flight. For both the in-plane and out-of-plane microphone positions a trend of increasing noise with increasing flow angle is observed for frequencies up to approximately 10 kHz. This increase in noise is due to the negative inflow increasing the unsteady loading. An opposite trend occurs above 10 kHz, which shows a decrease in broadband noise for increasing flow angle and is most apparent for the in-plane microphone where elevation angle is constant for a changing α_p.

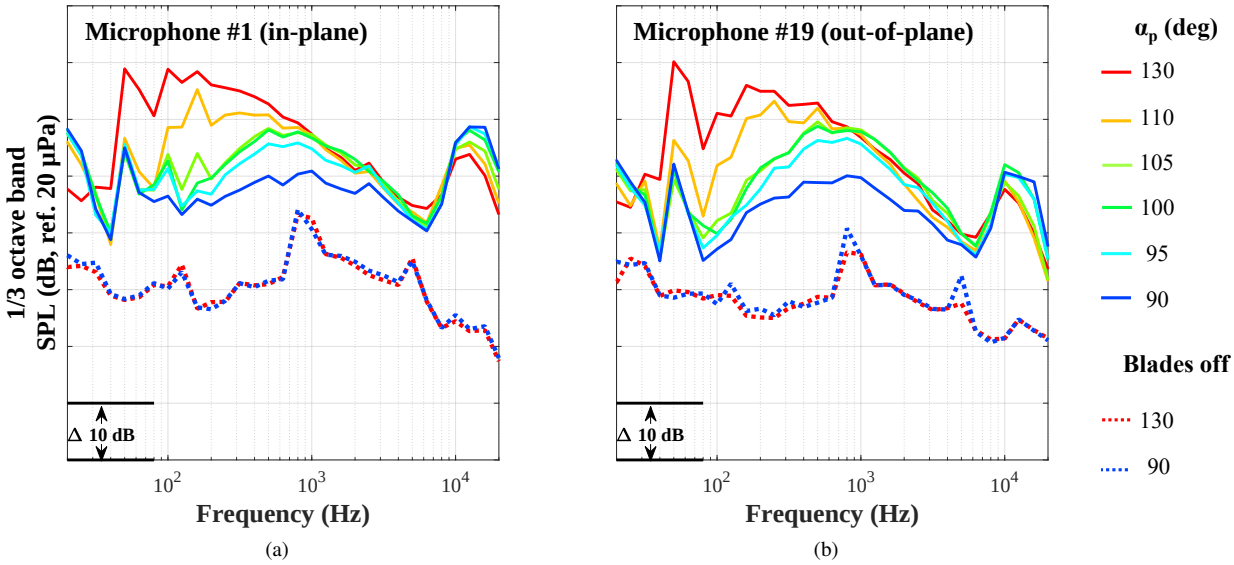

Fig. 12 Flow angle sweep at 10 m/s for a) in-plane microphone #1 and b) out-of-plane microphone #19 (V_∞ = 10 m/s, θ_0 = 11 degrees, α_p = 90 to 130 degrees).

A sweep on wind speed in the transition flight regime (α_p = 70 degrees) was performed for wind speeds of 10, 20, and 30 m/s for a constant RPM and θ_0 of 11 degrees, see Figs. 13a and 13b. Blades off noise is provided for each wind speed and increases with increase in wind speed. For this propeller, speeds above 10 m/s result in poor signal-to-noise particularly between 100 Hz and 5 kHz. For both microphones, there is an overall increase in the tonal and broadband noise with wind speed.

D. Unweighted and A-weighted Integrated Sound Pressure level Analysis

The unweighted and A-weighted integrated sound pressure levels (ISPL), integrated from 20 Hz to 20 kHz, are shown in Fig. 14a for the same blade pitch sweep as shown in Figs. 9a and 9b. ISPL trends for microphones #1 and #19 are presented as a function of increasing thrust on the x-axis and increasing ISPL on the y-axis. As shown in Fig. 9a, tonal noise was more prominent for the in-plane microphone and therefore the unweighted ISPL increases as thrust increases. However, the out-of-plane microphone, which had higher levels at mid-to-high frequencies (see Fig. 9b), demonstrates a noise minimum near the center of the thrust range. This noise bucket is also seen for both mics when using A-weighting, which puts more emphasis on the middle frequencies and less on the tonal noise at this condition.

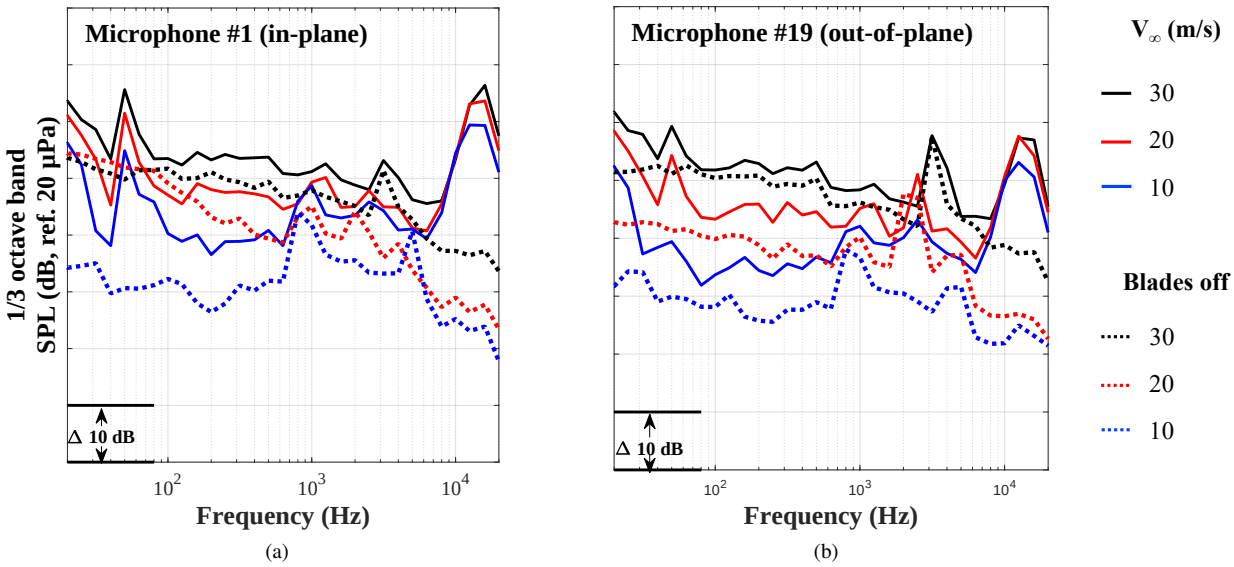

Fig. 13 Transition wind speed sweep for a) in-plane microphone #1 and b) out-of-plane microphone #19 (V_∞ = 10 to 30 m/s, θ_0 = 11 degrees, α_p = 70 degrees).

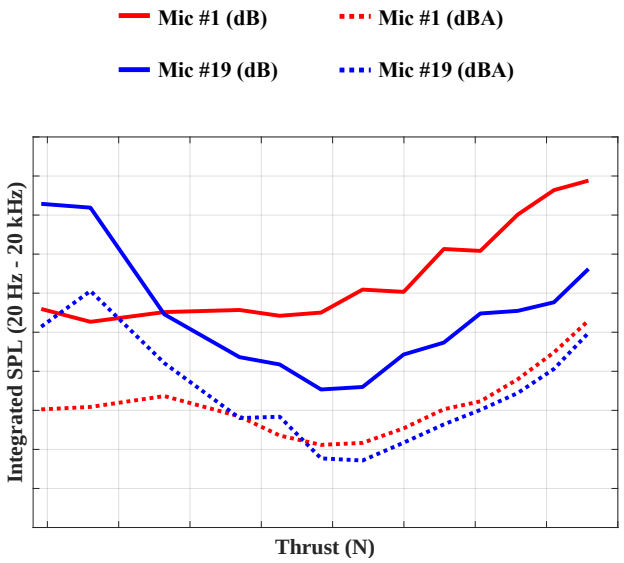

Fig. 14 Unweighted and A-weighted integrated sound pressure level as a function of thrust (increasing left to right) for a blade pitch sweep at constant RPM measured at an a) in-plane microphone #1 and b) out-of-plane microphone #19 (V_∞ = 0 m/s, θ_0 = -4 to 27 degrees, α_p = 0 degrees).

VI. Conclusion

An isolated Joby Aviation S4 propeller was tested in the NFAC 40- by 80-Foot Wind Tunnel to provide high quality performance, loads, and acoustic data to both the RVLT project and Joby Aviation. Test procedures and a sampling of results from the NASA RVLT acoustic portion of this test were presented. Information regarding test hardware, setup, data processing, and test matrix were provided. Preliminary results from the reflection tests, blades off noise, and main test were presented. While 20 strut-mounted microphones were recorded, only results from in-plane microphone #1 and out-of-plane microphone #19 were shown and discussed. Future work could focus on investigating the acoustic directivity and studying the noise source characteristics in greater detail.

The reflection tests revealed the presence of reflections at every microphone and turntable location, which could be attributed to reflective surfaces such as microphone/model strut hardware, camera ports, acoustic liner deterioration, and turntable acoustic liner limitations. Results from the test campaign were processed using the half-second spectral averaging method and presented in terms of 1/3 octave band spectra. Due to additional non-propeller noise sources (hardware cooling fan), a Vold-Kalman filter was applied to improve signal-to-noise between 500Hz and 10 kHz. Discussion of results highlighted trends in tonal, loading, and broadband noise due to the change in noise sources in specific frequency ranges. A sweep of blade pitch and RPM was performed in hover along with a with a study on the effect of constant thrust for varying RPM and blade pitch angles. Sweeps were performed in the transition and edgewise configuration for a flow angle sweep (α_p = 90 to 130 degrees) at 10 m/s and a wind speed sweep (V_∞ = 10 to 30 m/s) at α_p = 70 deg. Signal-to-noise ratio was poor for some frequencies at speeds above 10 m/s due to the NFAC fan drive system. Regardless, acoustic data for a variety of conditions for the Joby S4 propeller have been acquired and can be used for the validation of RVLT prediction tools. Validation of these tools will allow more confidence in the RVLT Conceptual Design Toolchain, benefiting the eVTOL community as a whole.

Acknowledgments

Authors would like to thank the Revolutionary Vertical Lift Technology project, Joby Aviation, and the entire NFAC test team. In particular, personnel and interns from the Aeromechanics Office at NASA Ames Research Center provided support for data acquisition and planning efforts. Furthermore, technical discussions and support between NASA Ames Research Center and NASA Langley Research Center provided guidance and support throughout the entire test campaign. Some key people include Benny Cheung, Kyle Pascioni, Nikolas Zawodny, Doug Boyd, Stefan Letica, Thomas Norman, James Stephenson, and Christopher Thurman. This paper is dedicated to the late Alex Stoll.

References

[1] Pascioni, K. A., Watts, M. E., Houston, M., Lind, A., Stephenson, J. H., and Bain, J., "Acoustic Flight Test of the Joby Aviation Advanced Air Mobility Prototype Vehicle," *28th AIAA/CEAS Aeroacoustics 2022 Conference*, AIAA, Southampton, UK, 2022.

[2] Weist, L., Schatzman, N., and Shirazi, D., "Best Practices for Predicting Acoustics of a Single Rotor Using the NASA RVLT Conceptual Design Toolchain," *2024 Transformative Vertical Flight Conference*, Santa Clara, CA, February 6-8, 2024.

[3] Soderman, P. T., Jaeger, S. M., Hayes, J. A., and Allen, C., "Acoustic Quality of the 40- by 80-Foot Wind Tunnel Test Section After Installation of a Deep Acoustic Lining," Tech. Rep. NASA TP-2002-211851, 2002.

[4] Schatzman, N., Weist, L., Hodge, M., Kyrychenko, D., Zhang, A., and Deng, S. K., "Aeroacoustic Measurements of the Bell 699 Rotor on the Tiltrotor Test Rig in the National Full-Scale Aerodynamics Complex 40-by 80-Foot Wind Tunnel," Tech. Rep. NASA TM-2019–220318, 2019.

[5] Stephenson, J. H., Schatzman, N. L., Cheung, B. K., Zawodny, N. S., Sargent, D. C., and Sim, B. W.-C., "Aeroacoustic Measurements from the Aerodynamic and Acoustic Rotorprop Test (AART) in the National Full-Scale Aerodynamics Complex (NFAC) 40-by 80-Foot Wind Tunnel," *The Vertical Flight Society's 77th Annual Forum and Technology Display*, Virtual, May 10–14, 2021.

[6] Schatzman (Barbely), N. L., Kitaplioglu, C., and Sim, B. W., "Acoustics Reflections of Full-Scale Rotor Noise Measurements in NFAC 40-by 80-Foot Wind Tunnel," *American Helicopter Society Specialists' Conference on Aeromechanics*, San Francisco, CA, January 20-22, 2010.

[7] Hutcheson, F. V., and Brooks, T. F., "Noise radiation from single and multiple rod configurations," *International Journal of Aeroacoustics*, Vol. 11, No. 3-4, 2012, pp. 291–333.

[8] McMasters, J., Nordvick, R., Henderson, M., and Sandvig, J., "Two Airfoil Sections Designed for Low Reynolds Number," *Technical Soaring*, Vol. 6, No. 4, 1981, pp. 2–24.

[9] *MATLAB user manual version 9.14.0.2206163 (R2023a)*, The MathWorks Inc., Natick, Massachusetts, 2023.

[10] Welch, P., "The use of fast Fourier transform for the estimation of power spectra: a method based on time averaging over short, modified periodograms," *IEEE Transactions on audio and electroacoustics*, Vol. 15, No. 2, 1967, pp. 70–73.

[11] Vold, H., and Leuridan, J., "High Resolution Order Tracking at Extreme Slew Rates Using Kalman Tracking Filters," *Noise and Vibration Conference and Exposition*, 1993.

[12] Pascioni, K. A., Thai, A. D., and Bain, J. J., "Propeller Source Noise Separation from Flight Test Measurements of the Joby Aviation Aircraft," *30th AIAA/CEAS Aeroacoustics 2024 Conference*, 2024.

[13] Thai, A. D., Bain, J. J., and Pascioni, K. A., "Identification and Computation of Individual Propeller Acoustics of the Joby Aviation Aircraft," *30th AIAA/CEAS Aeroacoustics 2024 Conference*, 2024.

[14] Bendat, J. S., and Piersol, A. G., *Random data: analysis and measurement procedures*, John Wiley & Sons, 2011.